Expression and purification of human neutrophil proteinase 3 from insect cells and characterization of ligand binding

Fahimeh Khorsand[1], Bengt Erik Haug[2,3], Inari Kursula[1,4,] Nathalie Reuter[2,5], and Ruth Brenk[1,5]*

[1]Department of Biomedicine, University of Bergen, Norway,

[2]Department of Chemistry, University of Bergen, Norway,

[3]Centre for Pharmacy, University of Bergen, Norway,

[4]Faculty of Biochemistry and Molecular Medicine, University of Oulu

[5]Computational Biology Unit, University of Bergen, Norway

*Corresponding author

Email: ruth.brenk@uib.no (RB)

Abstract

Neutrophil proteinase 3 (PR3) is an important drug target for inflammatory lung diseases such as chronic obstructive pulmonary disease and cystic fibrosis. Drug discovery efforts targeting PR3 require active enzyme for *in vitro* characterization, such as inhibitor screening, enzymatic assays, and structural studies. Recombinant expression of active PR3 overcomes the need for enzyme supplies from human blood and in addition allows studies on the influence of mutations on enzyme activity and ligand binding. Here, we report the expression of recombinant PR3 (rPR3) using a baculovirus expression system. The purification and activation process described resulted in highly pure and active PR3. The activity of rPR3 in the presence of commercially available inhibitors was compared with human PR3 by using a fluorescence-based enzymatic assay. Purified rPR3 had comparable activity to the native human enzyme, thus being a suitable alternative for enzymatic studies *in vitro*. Further, we established a surface plasmon resonance-based assay to determine binding affinities and kinetics of PR3 ligands. These methods provide valuable tools for early drug discovery aiming towards treatment of lung inflammation.

Introduction

Lung inflammation which occurs in diseases such as asthma, chronic obstructive pulmonary disease (COPD), cystic fibrosis (CF), and pneumonia is a serious challenge to public health worldwide (1). COPD, mainly caused by environmental factors, such as smoking, is projected to be the third leading cause of death by 2030 (2,3). Airway epithelial dysfunction and airway neutrophilic inflammation leading to airflow obstruction and impaired lung function are involved in the initiation and progress of clinical conditions associated with COPD and CF (4). As neutrophils migrate in response to an infection, serine proteases are released from their azurophil granules and play a major role in degrading proteins from pathogens but also target the extracellular matrix proteins to facilitate neutrophil migration (5).

37 Imbalance between these serine proteases and their endogenous inhibitors and increased protease
38 activity have a prominent role in the destruction of lung parenchyma (emphysema) (6) and as a result,
39 neutrophil serine proteases have been in focus as potential drug targets for the treatment of
40 inflammatory lung diseases.

41 The roles of the medically important serine proteases neutrophil elastase (hNE), cathepsin G (CatG),
42 and proteinase 3 (PR3) have been characterized in neutrophils. They are involved in a variety of
43 inflammatory human conditions, including chronic lung diseases, in addition to their involvement in
44 pathogen destruction and the regulation of proinflammatory processes (7). hNE has been the subject
45 of drug discovery studies for over 30 years (see e.g.(8,9)). Several inhibitors have been developed, and
46 some of them have been progressed to clinical studies, but only sivelestat (ONO-5046) has been
47 approved in some countries (Japan and South Korea) for the treatment of acute lung injury and
48 respiratory distress (10,11). Studies on some hNE inhibitors, such as ONO-6818, alvelestat (AZD9668),
49 and AZD6553, have been discontinued owing to unsatisfactory results from clinical trials (12). BAY-85-
50 8501 is a new highly potent hNE inhibitor and has been evaluated in a phase II trial for safety and
51 efficacy in patients with non-cystic fibrosis bronchodilation (13,14). While studies on hNE are still in
52 progress, another neutrophil serine protease, proteinase 3 (PR3), has drawn the attention as a drug
53 target over the recent years. Despite PR3 and hNE being homologues and sharing 56% sequence
54 identity, their ligand binding sites exhibit notable differences. The two enzymes have therefore slightly
55 different ligand and inhibitor selectivity, and existing drug candidates targeting hNE are not necessarily
56 also potent inhibitors of PR3 resulting in selective inhibition of some compounds (7,15). Yet, PR3 is a
57 promising drug target for COPD and CF for several reasons: higher levels of PR3 than hNE are released
58 from neutrophil azurophil granules, PR3 is active as both a membrane-bound and a free enzyme, PR3
59 is present in a larger area of the cell than hNE and local lung derived inhibitors have less impact on PR3
60 than hNE (16–18).

61 Owing to the importance of evaluating the potency of drug candidates against PR3, preparing a
62 sufficient amount of this enzyme for crystallization, binding assays, and activity screening is in high
63 demand. PR3 purification from neutrophils is a difficult and costly process with low yields. Expression
64 of recombinant PR3 (rPR3) in bacteria (19), yeast (19), insect cells (20,21), human mast cells (22), and
65 adherent 293 cells (23) have been used to study the recognition of rPR3 by anti-PR3 autoantibodies
66 (PR3-ANCA) or to study the processing of the amino- and carboxy-termini. However, production of
67 rPR3 for activity assays has not been reported.

68 Here, we aimed at to expressing active PR3 suitable for kinetic experiments and ligand studies. We
69 report the expression of rPR3 using *Spodoptera frugiperda* (Sf9) and the results of inhibition assays for
70 rPR3 and PR3 purified from neutrophils to compare the activities of these proteins. As information on
71 binding kinetics is of important for drug discovery (24), we also developed a surface plasmon
72 resonance (SPR) assay for the determination of binding affinities and kinetics of rPR3 inhibitors. The
73 developed methods provide an experimental framework to support drug discovery efforts for PR3.

74 Methods

75 Chemicals and reagents

76 All chemicals and reagents were of analytical grade. The elastase inhibitors selected for the inhibition
77 study of rPR3 were purchased from the following suppliers: α1-antitrypsin (Sigma-Aldrich), sivelestat
78 (Sigma-Aldrich), alvelestat (MedChemExpress), and BAY-85-8501 (MedChemExpress). Enzymes
79 purified from human neutrophiles (hPR3 and hNE) were purchased from Athens Research and
80 Technology. hNE substrate (MeOSuc-AAPV-AMC) was supplied by Santa Cruz Biotechnology. The FRET
81 peptide used as the PR3 substrate in enzymatic assay was prepared as described before (25).

82 Plasmids/vector constructs

83 Five constructs (P2-6, Figure 1) were synthesised and cloned in to the pFastBAC1 vector by Genscript.
84 The Mellitin signal sequence to direct secretion of the expressed protein (26) was inserted upstream

85 of the PR3 sequence (either the sequence for the whole protein or the mature protein) followed by a
86 TEV cleavage site and either a His-tag or Strep-tag (see supplementary material for the DNA sequences
87 of the different constructs).

88 Bacmid and baculovirus preparation

89 Bacmids were generated using the EMBacY MultiBac system (Geneva Biotech). Genes of interest were
90 inserted into bacmids by Tn7 transposition. DH10EMBacY competent *E. coli* (EMBL, Grenoble), which
91 contained both the EMBacY genome (bacmid) and the helper plasmid (IPTG inducible
92 Tn7 transposon complex with tetracycline resistance gene), were transformed with pFastBac1 vectors
93 containing the genes for the different PR3 constructs and plated onto selection agar plates. Positive
94 colonies were selected based on blue/white screening and the bacmid was purified for transfection
95 and virus production in Sf9 insect cells. Bacmids containing the PR3 sequences were isolated and
96 checked by PCR with M13 primers to make sure that the size of the bacmids was the same as expected
97 (see supplementary material, Fig S1a).

98 Expression of rPR3

99 Recombinant protein was expressed in baculovirus-infected insect cells using the protocol described
100 by Bieniossek *et al.* (27). Sf9 cells (Invitrogen) were transfected with the bacmid, using the FuGENE®6
101 transfection reagent (Promega), and virus particles were harvested after 7 d of infection. The
102 recombinant primary virus was amplified to a high-titre viral stock. Approximately 9 µl (1×10^6 cells)
103 of the high-titre virus were used to infect the insect-cell culture at a cell density of 0.6–0.8 ×
104 10^6 cells/mL. The culture was centrifuged at 7000 g for 30 min after 5 d, and the supernatant (clarified
105 expression medium) was filtered with 0.45 µm sterile filters and used for protein purification.

106 Monitoring of rPR3 expression

107 To monitor expression of rPR3, 15 mL samples were collected 24, 48, and 72 h after the Sf9 cells
108 infected with baculoviruses made with the different constructs reached growth arrest. The culture was

109 centrifuged at 1000 g for 15 min, the cleared medium was concentrated 30 times to the final volume
110 of 500 µL and was stored at -20 °C. The pellet was resuspended in 300 µL PBS and stored at -20 °C. To
111 perform the dot blot, samples were thawed. The cells were centrifuged to remove PBS and resuspend
112 with the lysis buffer (50 mM Tris-HCl, pH 8 with 50 mM NaCl, protease inhibitor). 2 µL from the
113 supernatant and cell lysates were applied on a nylon membrane and two different antibodies (an HRP-
114 conjugated anti-His tag from Qiagen and an HRP-conjugated anti-strep tag from Sigma-Aldrich) were
115 used on separate blots to detect PR3. The metal enhanced DAB substrate kit (ThermoScientific) was
116 used for staining of the blots.

117 Purification

118 The supernatant from 5-10 L culture was loaded on an HisTrap Excel column (Cytiva) overnight and
119 washed for 20-30 column volumes with buffer A (50 mM potassium phosphate, 150 mM NaCl, pH 7.4).
120 Another washing step was carried out with buffer B (buffer A plus 50 mM imidazole) for 10 column
121 volumes, and the protein was eluted with a gradient of 50 to 400 mM imidazole in buffer A over 10
122 column volumes. The eluted protein was concentrated and loaded on a SEC200 increase 10/300
123 column (Cytiva), and was eluted using buffer C (50 mM sodium acetate, 150 mM NaCl, pH 5.5). The
124 identity of the purified protein was confirmed using mass spectrometry (Fig S1c).

125 Activation of rPR3

126 To cut off the N-terminal dipeptide from PR3 and activate the enzyme, purified rPR3 and cathepsin C
127 (Sigma-Aldrich C8511) were mixed at a ratio of 95:5 in the activation buffer (5 mM mercaptoethanol
128 in buffer C) and incubated at 35 °C for 18 h.

129 Enzymatic activity assay

130 The enzymatic assay is similar to the one we reported earlier (28) with minor modifications. Briefly, to
131 determine the inhibition of PR3, 0.25 nM of enzyme was incubated with buffer (50 mM HEPES pH 7.4,
132 750 mM NaCl, 0.5% Igepal and 1% DMSO) or buffer containing the inhibitors at various concentrations

133 for 30 min at RT. The reaction was started by adding the FRET peptide (Abz-VADnVADYQ-EDDnp) at a
134 final concentration of 5 μM. The fluorescent signal (excitation filter 320, emission filter 420) was read
135 every 30 s for 30 min at 30 °C with a fluorescent plate reader (Tecan Spark) and the enzymatic activity
136 was measured from the initial linear portion of the slope (fluorescent signal/min) of the time-course
137 curve of reaction progress.

138 For the activity assay with hNE, 0.25 nM of enzyme was incubated as described above for PR3. The
139 reaction was started by adding the fluorogenic substrate (MeOSuc-AAPV-AMC) at a final concentration
140 of 5 μM. The fluorescent signal (excitation filter 360, emission filter 460) was read as described above
141 for PR3.

142 Data were fitted using nonlinear regression analysis (GraphPad Prism v.9) to determine the IC_{50} values.

143 Biotinylation of rPR3

144 50 μL activated rPR3 (2 mg/mL) in PBS was mixed with NHS-PEG4-Biotin at a molar excess of 20-fold
145 and incubated at RT for 30 min. Unreacted biotin was removed by 4 times diluting and concentrating
146 the buffer so that the final concentration was 1/10000 of the starting concentration. Biotinylation was
147 confirmed using a chromogenic detection kit (Thermo ScientificTM).

148 SPR assay

149 The SPR data were obtained using a Biacore T200 (GE Healthcare Life Sciences) and presented as the
150 mean of triplicate measurements. Briefly, 100 μL of 200 nM biotinylated rPR3 in PBS was injected and
151 captured on a NAHLC 1500M chip (XanTec Bioanalytics GmbH) at a flow rate of 5 μL/min. Biotinylated
152 protein was captured to an immobilization level of around 4000-8000 RU. As reference, an unrelated
153 protein available in our group, biotinylated δMtDXR (*Mycobacterium tuberculosis* 1-deoxy-D-xylulose
154 5-phosphate reductoisomerase) expressed in BL21(DE3) *E. coli* cells and biotinylated enzymatically
155 with GST-BirA, was immobilized on the reference flow cell (3500-4000 RU). The running buffer for the
156 immobilization of the proteins was PBSP (GE Healthcare Life Sciences). The binding assay was carried

157 out using the same buffer and a flow rate of 30 µL/min at 25 °C. To measure compound binding,
158 different concentrations of the studied compounds were injected for 200-300 s over the flow cells
159 starting with the lowest concentration and dissociation was initiated with the injection of the running
160 buffer which continued for 600-900 s. For regeneration, 1M NaCl was injected for 1 min. Sensorgrams
161 were double-referenced by subtracting the signal from a reference surface and the signal from one
162 blank injection. The Biacore T200 Evaluation Software 3.0 was applied for the determination of steady
163 state affinity and all the kinetic data using a global fit. K_D values were determined using an equation
164 corresponding to a reversible, one-step, 1:1 interaction model and fitting values taken at the end of
165 the injection (representing steady-state signals) by nonlinear regression analysis.

166 Results and discussion

167 rPR3 expression and purification

168 As a baculovirus expression system has been previously used to produce recombinant PR3 which
169 yielded the only available crystal structure so far (20), and as a eukaryotic expression system is needed
170 for posttranslational modifications (mainly glycosylations) and for the removal of preprosequences, we
171 opted for using *Spodoptera frugiperda* (Sf9) for recombinant expression of PR3. Five different
172 constructs were made for the expression of rPR3 (Fig 1, see Supporting information for sequences).
173 The mature PR3 sequence lacking both the N- and C-terminal preprosequences and the Ala-Glu
174 dipeptide from the propeptide was used in the constructs P5 and P6 while the whole PR3 sequence
175 was inserted in the constructs P2-4. The N-terminal propresequence of PR3 functions as the
176 endogenous signal peptide. All constructs contained a melittin signal peptide at the N-terminus to
177 direct the protein through the post-translational modification and secretory pathway as previously
178 described (19). Two types of affinity tags were investigated, a 6x His- tag either at the N-terminal (P5)
179 or at the C-terminal (P4 and P7), and a C-terminal Twin-Strep-tag (P2, P3 and P6). All constructs also

180 contained a TEV cleavage site between the PR3 sequence and the affinity tag to enable cleavage of the
181 tag if required.

182

183 **Fig 1- The different rPR3 constructs used in this study.** A melittin signal sequence (*Mel ss,* marked as
184 blue box) and a TEV cleavage site (black box) were included in all constructs. Three constructs
185 contained a C-terminal Strep-tag (P2, P3, and P6, purple box), a C-terminal His-tag (P4, pink box) or an
186 N-terminal His-tag (P5). In addition to the sequence for the mature PR3 (green box), three constructs
187 contained the N-terminal pre-peptide (P2-4, N- in green box) and two the C-terminal propeptide (P2
188 and P4, C- in green box).

189 Expression of the different constructs was monitored by measuring the fluorescence of YFP (yellow
190 fluorescent protein) which was co-expressed in the insect cells. YFP became visible after around 48 h
191 post-infection indicating that infection had been successful for all constructs (Fig S1b).

192 To determine if the different proteins were secreted into the media, we used anti-His and with anti-
193 Strep-tag antibodies. For the constructs P2, P3, P4 and P6 protein was clearly detectable in the lysate
194 and for P2, P3 and P4 protein was also detectable in the media (Fig 2). This indicates that the N-
195 terminal preprosequence of PR3 (endogenous signal peptide) is essential for the secretion of protein
196 to the medium. As the post-translational modifications are associated with the secretory pathway, we
197 considered secreted rPR3 to be of higher interest than non-secreted rPR3. Accordingly, the constructs
198 lacking the N-terminal preprosequence of PR3 (P5 and P6) were not considered for further studies.
199 Given the high cost associated with using Strep-Tactin columns for purification of Strep-tag containing
200 proteins and apparently similar expression levels for secreted proteins containing either a Strep-tag
201 (P2 and P3) or a His-tag (P4), we decided to continue further work with the construct containing a His-
202 tag.

203

204 **Fig 2- Dot blot analysis of rPR3 expression.** The time given refers to the time the sample was taken
205 after cell growth arrest was reached. Blot a was treated with an anti-His antibody and blot b with and
206 anti-Strep-tag antibody.

207

208 Subsequently, rPR3 obtained using construct P4 was purified. Purification of rPR3 with a His-trap
209 column resulted in a purity of approximately 80% (Fig. 3). Therefore, size exclusion chromatography
210 column was subsequently used to obtain pure rPR3. The purity of rPR3 was very high at this stage (Fig.
211 3) and the protein yield was around 400 μg/L of culture medium. The identity of rPR3 was confirmed
212 using mass spectrometry (Fig S1c and d).

213

214 **Fig 3- SDS-PAGE showing the purity of rPR3**. Purification was carried out with an Excel His-trap column
215 (lane His-trap) and in addition with a SEC200 column (lane SEC200).

216

217 In the next step, rPR3 was activated and the activity of the mature enzyme was assessed. To activate
218 rPR3, the N-terminal dipeptide needs to be removed (20). Here, this was achieved by treating PR3 with
219 cathepsin C. To determine the activity of the mature enzyme, a kinetic assay was conducted. Due to
220 ease of use, we opted to use an activity assay with a fluorogenic substrate. However, it is not possible
221 to determine kinetic parameters with this assay as this would lead to a too high background
222 fluorescence signal. Therefore, we have assessed the activity by comparing IC_{50} values of some potent
223 elastase inhibitors determined with hPR3 and rPR3 (Table 1). One of these inhibitors is α1-antitrypsin,
224 an endogenous serine protease inhibitor, also denoted SERPIN, which plays an important role in
225 balancing the activity of serine proteases in the body (29). The other three inhibitors are small
226 molecule hNE inhibitors that have been developed by various pharmaceutical companies over recent
227 years. For some of the compounds no inhibition data for PR3 is available. To allow comparison to

228 literature values, we therefore determined also the IC_{50} values of these compounds for hNE (Table 1).
229 Indeed, the obtained values of these inhibitors against hNE were comparable with the data available
230 in literature giving confidence in the assay setup (Table 1, Fig S2). For alvelestat, enzyme inhibition
231 could not be determined up to 2.5 μM. Measuring higher concentrations was not possible due to high
232 background fluorescence. For the remaining compounds, very similar IC_{50} values for hPR3 and rPR3
233 were obtained (Table 1, Fig S2). These data show that we were able to produce rPR3 with similar
234 activity as hPR3.

235 **Table 1- IC_{50} values for known elastase and PR3 inhibitors determined using hPR3, rPR3 and hNE.**

		IC_{50} [nM]*			
		hNE			
Inhibitor	**Structure**	**This study**	**Literature value (reference)**	**hPR3**	**rPR3**
BAY-85-8501	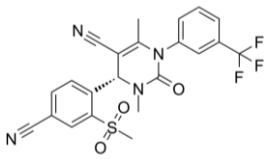	0.07 ± 0.01	0.065 (14)	27 ± 4	59 ± 8
Alvelestat	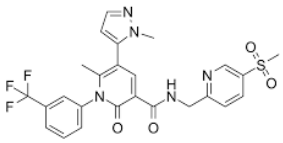	12 ± 1	12 (30)	N.D.**	N.D.**
Sivelestat	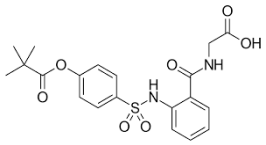	9 ± 1	44 (10)	33 ± 2	32 ± 4
α1-antitrypsin		0.5 ± 0.03	Ki < 0.1 (31)	15 ± 1	14 ± 1

236 *The IC_{50} values are presented as mean ± SD (n = 3).

237 ** N.D. : not determined due to high background fluorescence.

238

239 ## SPR assay to determine binding affinities and kinetics of PR3 inhibitors

240 Next, we developed a binding assay for rPR3 using SPR. This method allows for determination of both
241 binding affinities and kinetic parameters. Further, the SPR read-out is not influenced by fluorescence
242 interference from test compounds, thus this method should therefore also allow for measurement of
243 fluorescent compounds like alvelestat (Table 1). The assay was developed using neutravidin coated SPR
244 chips. Neutravidin is a non-glycosylated analogue of avidin (32) and allows for capture and
245 immobilization of biotinylated ligands onto the SPR chip. Accordingly, rPR3 was biotinylated with NHS-
246 PEG4-biotin which reacts with primary amines such as the side chain of lysine residues or the amino-
247 termini of polypeptides. The injection of biotinylated rPR3 into the flow cell led to high and stable
248 binding to the chip (Fig S3). As reference, an unrelated protein available in our laboratory, biotinylated
249 δMtDXR was selected and immobilized in the reference cell (Fig S3). The binding sites of rPR3 and DXR
250 are very different, thus affinity of the investigated rPR3 inhibitors towards DXR was not expected. The
251 inhibitors were injected in a range of concentrations and binding responses were analysed (Fig 4).

252

253 **Fig 4- Sensorgrams of (a) BAY-85-8501, (b) alvelestat, (c) sivelestat, and (d) α1-antitrypsin binding to**
254 **rPR3.**

255

256 For BAY-85-8501, a K_D of 47 nM was determined using steady state kinetics and a K_D of 14 nM using
257 flow kinetics (Fig 4a, Fig S3a, Table 2). These values are comparable to the K_i value of 50 nM derived
258 from the IC_{50} value for this compound (Table 1) using the Cheng-Prusoff equation ($K_i = IC_{50}/(1+ [S]/K_m)$)
259 and the literature K_M value of 27.4 µM (25). Using the 1:1 binding kinetic model, k_{on} and k_{off} rates were
260 also obtained (Table 2). Using these values, the residence time of this molecule was calculated to be
261 5.2 min.

262

263 **Table 2 – Binding affinities and kinetic parameters of rPR3 inhibitors determined using SPR.**

Compound	K_D (μM)	k_{on} (1/Ms)	k_{off} (1/s)	Steady state K_D (μM)
BAY-85-8501	(0.14 ± 0.03) x 10^{-1}	(2.25 ± 0.65) x 10^{+5}	(3.19 ± 1.5) x 10^{-3}	0.03 ± 0.01
Alvelestat	N.D.	N.D.	N.D.	13.5 ± 5.6

264 N.D. not determined because the data could not be fitted.

265 The reported values are the averages and SDs of triplicates.

266

267 When testing alvelestat in the SPR assay, we found it to be a weak rPR3 binder with fast association
268 and dissociation rates (Fig 3b). Therefore, the binding constant could only be determined using the
269 steady state method (Fig S3b) resulting in a K_D value of 13.5 μM (Table 2). This value is about 100 times
270 higher than the IC_{50} value determined for the same compound with hNE while no affinity could be
271 determined using the enzymatic assay (Table 1). The observed selectivity profile is in line with previous
272 data (30).

273 We found that sivelestat and α1-antitrypsin hardly dissociated from rPR3 (Fig4c and d), which is
274 consistent with the reported covalent binding capabilities of both these inhibitors (33,34). Inhibition
275 of PR3 by α1-antitrypsin is reported to take place in at least two steps: the enzyme and the inhibitor
276 first form a high-affinity reversible inhibitory complex EI* with an equilibrium dissociation constant
277 K^*_i of 38 nM and then EI* subsequently transforms into an irreversible complex EI with a first-order
278 rate constant k_2 of 0.04 s^{-1} (34). Sivelestat has been reported to covalently inhibit hNE via acylation
279 through formation of a pivaloyl ester (30).

280 Conclusion

281 Here, we report a protocol for expression of rPR3. The protein was subsequently used for
282 determination of ligand binding affinity and kinetics with SPR and inhibitor potency with a

fluorescence-based inhibition assay. We have demonstrated that the activity of rPR3 is comparable with the wild-type human neutrophil PR3 making it suitable to study ligand binding and inhibition. Our protocol is also suitable to produce mutant variants of PR3 which will allow further investigation of PR3 structure-activity relationship in inhibitor binding. Such studies will be highly valued to shed light on what drives ligand affinity and selectivity, as for example here observed for alvelestat (Tables 1 and 2), especially as no crystal structures of PR3-inhibitor complexes are currently available. We have also developed an SPR-based protocol which can be used to determine binding affinity (K_D) and kinetic constants The SPR data was in line with the inhibition data obtained using a fluorogenic enzymatic assay confirming the efficacy and accuracy of the SPR data to characterize ligand binding. Collectively, the reported methods will we very valuable tools to support drug discovery endeavours towards PR3.

Acknowledgement

The work was supported by the Research Council of Norway (RESPOND3, grant number 294594). We made use of the Facility for Biophysics, Structural Biology and Screening at the University of Bergen (BiSS), which has received funding from the Research Council of Norway (RCN) through the NORCRYST (grant number 245828) and NOR-OPENSCREEN (grant number 245922) consortia. We would like to thank Bruna Schuck de Azevedo for providing us with the biotinylated MtDXR used in the SPR assay. MS data was collected at the Mass spectrometry core facility at the University of Oulu.

References

1. Moldoveanu B, Otmishi P, Jani P, Walker J, Sarmiento X, Guardiola J, et al. Inflammatory mechanisms in the lung. J Inflamm Res. 2009;2:1–11.

2. Brandsma C, Van den Berge M, Hackett T, Brusselle G, Timens W. Recent advances in chronic obstructive pulmonary disease pathogenesis: from disease mechanisms to precision medicine. J Pathol. 2020 Apr;250(5):624–35.

3. Mathers CD, Loncar D. Projections of global mortality and burden of disease from 2002 to 2030. PLOS Med. 2006 Nov 28;3(11):e442.

308 4. De Rose V, Molloy K, Gohy S, Pilette C, Greene CM. Airway epithelium dysfunction in cystic fibrosis
309 and COPD. Mediators Inflamm. 2018 Apr 8;2018:e1309746.

310 5. Pham CTN. Neutrophil serine proteases fine-tune the inflammatory response. Int J Biochem Cell
311 Biol. 2008 Jun 1;40(6):1317–33.

312 6. Pandey KC, De S, Mishra PK. Role of proteases in chronic obstructive pulmonary disease. Front
313 Pharmacol. 2017 Aug 8;8:512.

314 7. Korkmaz B, Horwitz MS, Jenne DE, Gauthier F. Neutrophil elastase, proteinase 3, and cathepsin G
315 as therapeutic targets in human diseases. Sibley D, editor. Pharmacol Rev. 2010 Dec 1;62(4):726–
316 59.

317 8. Tsai YF, Hwang TL. Neutrophil elastase inhibitors: a patent review and potential applications for
318 inflammatory lung diseases (2010 – 2014). Expert Opin Ther Pat. 2015 Oct 3;25(10):1145–58.

319 9. Crocetti L, Quinn MT, Schepetkin IA, Giovannoni MP. A patenting perspective on human neutrophil
320 elastase (HNE) inhibitors (2014-2018) and their therapeutic applications. Expert Opin Ther Pat.
321 2019 Jul;29(7):555–78.

322 10. Kawabata K, Suzuki M, Sugitani M, Imaki K, Toda M, Miyamoto T. ONO-5046, a novel inhibitor of
323 human neutrophil elastase. Biochem Biophys Res Commun. 1991 Jun 14;177(2):814–20.

324 11. Hagiwara S, Iwasaka H, Togo K, Noguchi T. A neutrophil elastase inhibitor, sivelestat, reduces lung
325 injury following endotoxin-induced shock in rats by inhibiting HMGB1. Inflammation. 2008 Aug
326 1;31(4):227–34.

327 12. Ti H, Zhou Y, Liang X, Li R, Ding K, Zhao X. Targeted treatments for chronic obstructive pulmonary
328 disease (COPD) using low-molecular-weight drugs (LMWDs). J Med Chem. 2019 Jul
329 11;62(13):5944–78.

330 13. Von Nussbaum F, Li VM, Meibom D, Anlauf S, Bechem M, Delbeck M, et al. Potent and selective
331 human neutrophil elastase inhibitors with novel equatorial ring topology: in vivo efficacy of the
332 polar pyrimidopyridazine BAY-8040 in a pulmonary arterial hypertension rat model.
333 ChemMedChem. 2016;11(2):199–206.

334 14. Von Nussbaum F, Li VMJ, Allerheiligen S, Anlauf S, Bärfacker L, Bechem M, et al. Freezing the
335 bioactive conformation to boost potency: The identification of BAY 85-8501, a selective and potent
336 inhibitor of human neutrophil elastase for pulmonary diseases. ChemMedChem.
337 2015;10(7):1163–73.

338 15. Hajjar E, Broemstrup T, Kantari C, Witko-Sarsat V, Reuter N. Structures of human proteinase 3 and
339 neutrophil elastase – so similar yet so different. FEBS J. 2010;277(10):2238–54.

340 16. Crisford H, Sapey E, Stockley RA. Proteinase 3; a potential target in chronic obstructive pulmonary
341 disease and other chronic inflammatory diseases. Respir Res. 2018 Sep 20;19(1):180.

342 17. Korkmaz B, Jaillet J, Jourdan ML, Gauthier A, Gauthier F, Attucci S. Catalytic activity and inhibition
343 of Wegener antigen proteinase 3 on the cell surface of human polymorphonuclear neutrophils. J
344 Biol Chem. 2009 Jul 24;284(30):19896–902.

345 18. Sinden NJ, Stockley RA. Proteinase 3 activity in sputum from subjects with alpha-1-antitrypsin
346 deficiency and COPD. Eur Respir J. 2013 May 1;41(5):1042–50.

19. Van der Geld YM, Oost-Kort W, Limburg PC, Specks U, Kallenberg CGM. Recombinant proteinase 3 produced in different expression systems: recognition by anti-PR3 antibodies. J Immunol Methods. 2000 Oct 20;244(1):117–31.

20. Fujinaga M, Chernaia MM, Halenbeck R, Koths K, James MNG. The crystal structure of PR3, a neutrophil serine proteinase antigen of Wegener's granulomatosis antibodies. J Mol Biol. 1996 Aug 16;261(2):267–78.

21. Van der Geld YM, Smook MLF, Huitema MG, Harmsen MC, Limburg PC, Kallenberg CGM. Expression of recombinant proteinase 3, the autoantigen in Wegener's granulomatosis, in insect cells. J Immunol Methods. 2002 Jun 1;264(1):195–205.

22. Specks U, Wiegert EM, Homburger HA. Human mast cells expressing recombinant proteinase 3 (PR3) as substrate for clinical testing for anti-neutrophil cytoplasmic antibodies (ANCA). Clin Exp Immunol. 1997;109(2):286–95.

23. Capizzi SA, Viss MA, Hummel AM, Fass DN, Specks U. Effects of carboxy-terminal modifications of proteinase 3 (PR3) on the recognition by PR3-ANCA. Kidney Int. 2003 Feb 1;63(2):756–60.

24. Knockenhauer KE, Copeland RA. The importance of binding kinetics and drug–target residence time in pharmacology. Br J Pharmacol [Internet]. 2023 [cited 2023 Sep 17];1–14(n/a). Available from: https://onlinelibrary.wiley.com/doi/abs/10.1111/bph.16104

25. Narawane S, Budnjo A, Grauffel C, Haug BE, Reuter N. In silico design, synthesis, and assays of specific substrates for proteinase 3: influence of fluorogenic and charged groups. J Med Chem. 2014 Feb 13;57(3):1111–5.

26. Tessier DC, Thomas DY, Khouri HE, Laliberié F, Vernet T. Enhanced secretion from insect cells of a foreign protein fused to the honeybee melittin signal peptide. Gene. 1991 Feb 15;98(2):177–83.

27. Bieniossek C, Richmond TJ, Berger I. MultiBac: Multigene baculovirus-based eukaryotic protein complex production. Curr Protoc Protein Sci. 2008;51(1):5.20.1-5.20.26.

28. Budnjo A, Narawane S, Grauffel C, Schillinger AS, Fossen T, Reuter N, et al. Reversible ketomethylene-based inhibitors of human neutrophil proteinase 3. J Med Chem. 2014 Nov 26;57(22):9396–408.

29. Janciauskiene S, Wrenger S, Immenschuh S, Olejnicka B, Greulich T, Welte T, et al. The multifaceted effects of alpha1-antitrypsin on neutrophil functions. Front Pharmacol. 2018 Apr 17;9:341.

30. Stevens T, Ekholm K, Gränse M, Lindahl M, Kozma V, Jungar C, et al. AZD9668: pharmacological characterization of a novel oral inhibitor of neutrophil elastase. J Pharmacol Exp Ther. 2011 Oct 1;339(1):313–20.

31. Von Nussbaum F, Li VMJ. Neutrophil elastase inhibitors for the treatment of (cardio)pulmonary diseases: Into clinical testing with pre-adaptive pharmacophores. Bioorg Med Chem Lett. 2015 Oct;25(20):4370–81.

32. Sut TN, Park H, Koo DJ, Yoon BK, Jackman JA. Distinct binding properties of neutravidin and streptavidin proteins to biotinylated supported lipid bilayers: implications for sensor functionalization. Sensors. 2022 Jan;22(14):5185.

33. Nakayama Y, Odagaki Y, Fujita S, Matsuoka S, Hamanaka N, Nakai H, et al. Clarification of mechanism of human sputum elastase inhibition by a new inhibitor, ONO-5046, using electrospray ionization mass spectrometry. Bioorg Med Chem Lett. 2002 Sep 2;12(17):2349–53.

34. Duranton J, Bieth JG. Inhibition of proteinase 3 by α1-antitrypsin in vitro predicts very fast inhibition in vivo. Am J Respir Cell Mol Biol. 2003 Jul;29(1):57–61.

392 # Supporting information

393 All the DNA sequences and the corresponding protein sequences for the vector constructs P2-6 can be
394 found in the supplementary material. The M13 primers sequence is also available in the
395 supplementary material file. Additionally, the supporting information contains the four following
396 figures:

397 **Fig S1- Expression and identification of rPR3 in insect cells.** a) Agarose gel to detect bacmid
398 production. b) Sf9 cells infected with baculovirus showing expression of YFP as green dots using
399 fluorescent microscopy. c) MALDI-ToF mass spectrum of rPR3, the measured mass and the sequence
400 range is written above the peaks and the colours match the colours of amino acids in the rPR3
401 sequence showed in (d).

402 **Fig S2- Dose-response curves of inhibitors BAY-85-8501, sivelestat, and α1antitrypsin measured with**
403 **hNE, hPR3, and rPR3.** The activity measurements for each compound concentration were conducted
404 in duplicates or triplicates. For a given inhibitor, each data point on the curve represents the average
405 of two or three replicates and the error bars represent the standard deviation. The relative activity is
406 the ratio of enzymatic activity in the presence of inhibitor to the activity of enzyme in the absence of
407 the inhibitor. The non-linear fit was performed using GraphPad Prism® with a non-linear fit with a
408 standard slope (Hill slope = -1).

409 **Fig S3- Immobilization of biotinylated rPR3 (a) on the flow cell 2 and (b) the reference protein**
410 **δMtDXR on the flow cell 1 of a NAHLC SPR chip.** Injection of protein was followed by washing the
411 unbound protein with the running buffer. In the reference flow cell, a second injection was carried out
412 for a shorter period to increase the protein binding level on the flow cell 1.

413 **Fig S4– Analysis of sensorgrams to determine K_D values.** Steady state analysis of sensorgrams for BAY-
414 85-8501 (a, K_D = 0.03 ± 0.001 μM) and alvelestat (b, K_D = 13.5 ± 5.6 μM) binding to rPR3. c) Fitting of
415 BAY85-8501 sensorgrams to the 1:1 ligand binding model for the kinetics analysis with Biacore

416 evaluation software. All graphs were created from data from a single experiment using the Biacore

417 T200 Evaluation Software 3.0 .

418

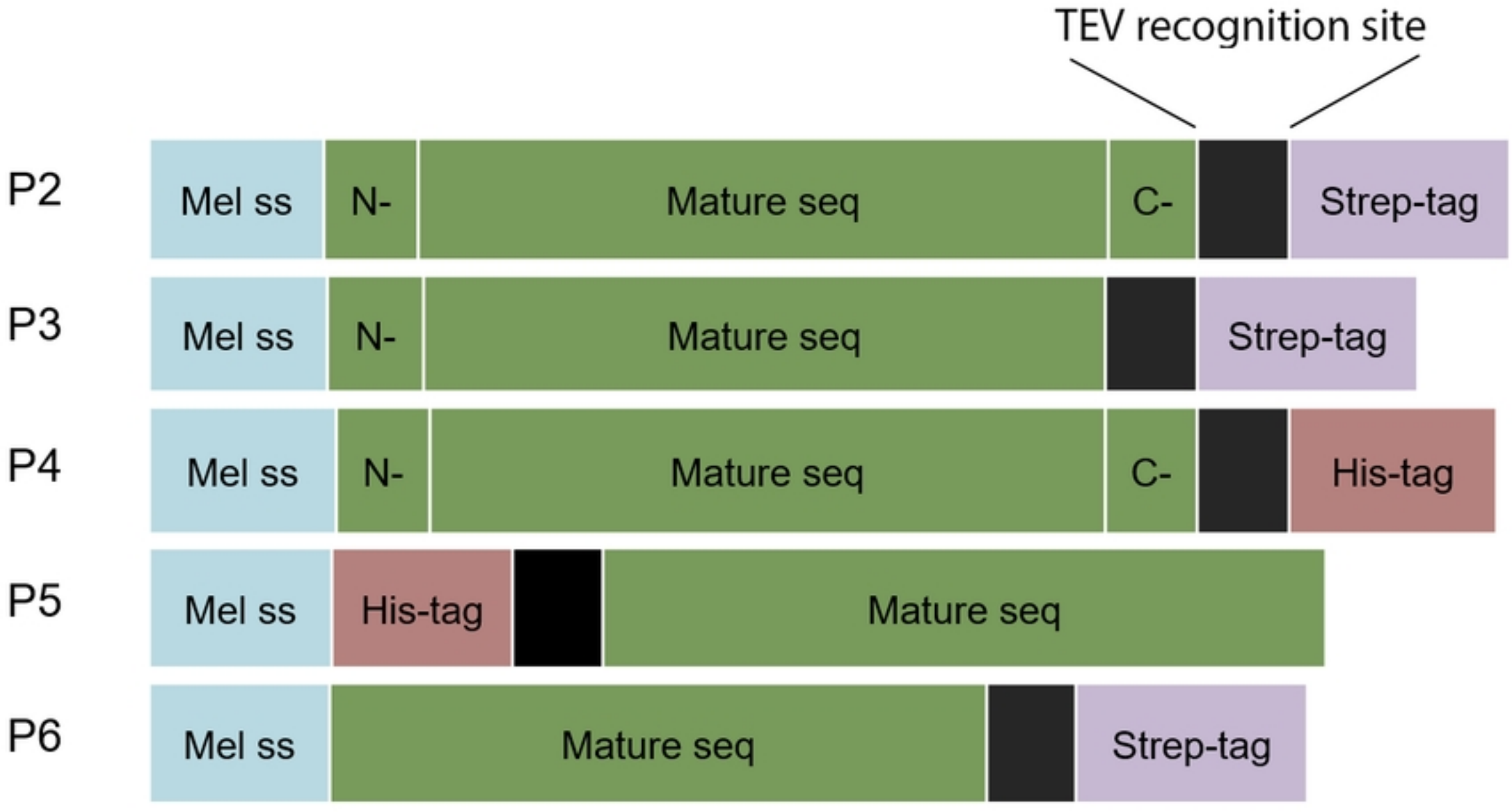
TEV recognition site
P2
Mel ss
N-
Mature seq
C-
Strep-tag
P3
Mel ss
N-
Mature seq
Strep-tag
P4
Mel ss
N-
Mature seq
C-
His-tag
P5
Mel ss
His-tag
Mature seq
P6
Mel ss
Mature seq
Strep-tag

Figure 1

a

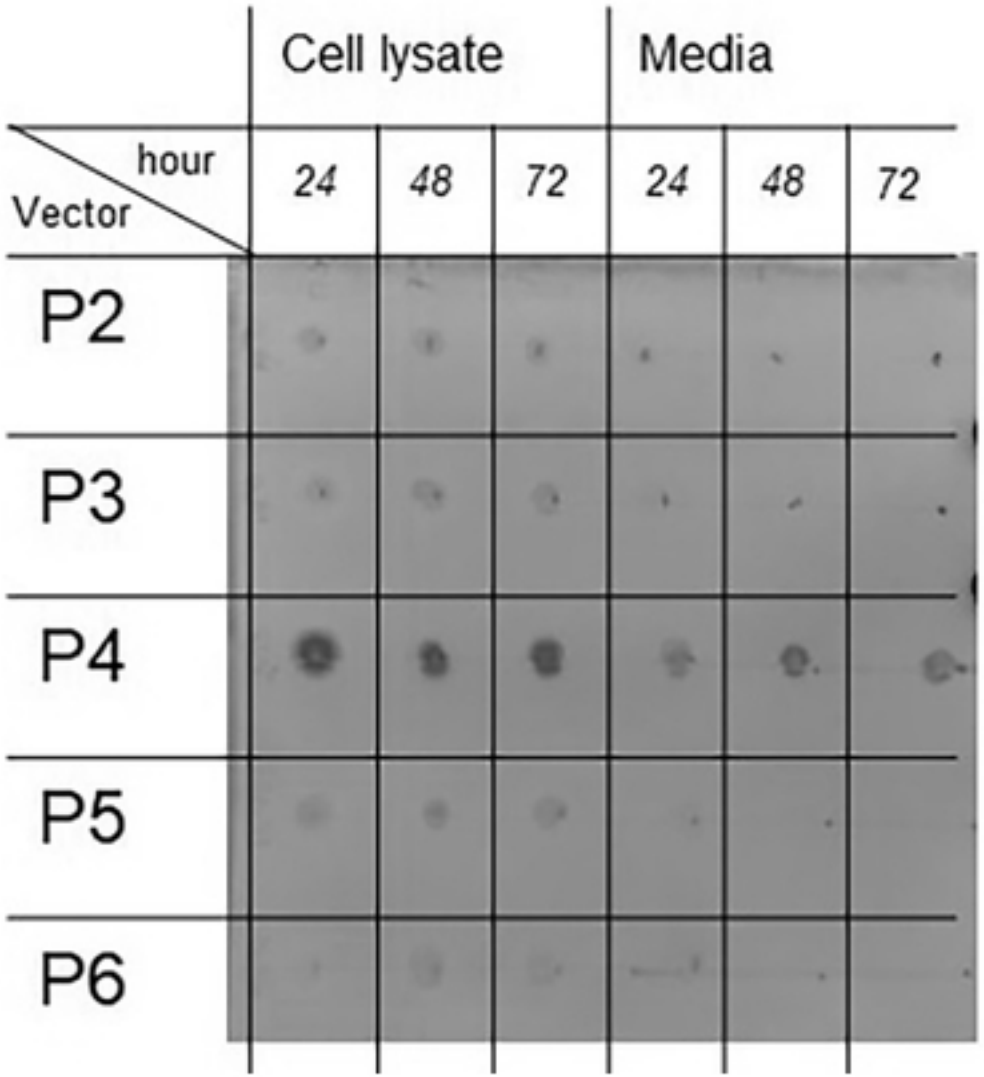
Cell lysate
Media
hour
Vector
24
48
72
24
48
72
P2
P3
P4
P5
P6

b

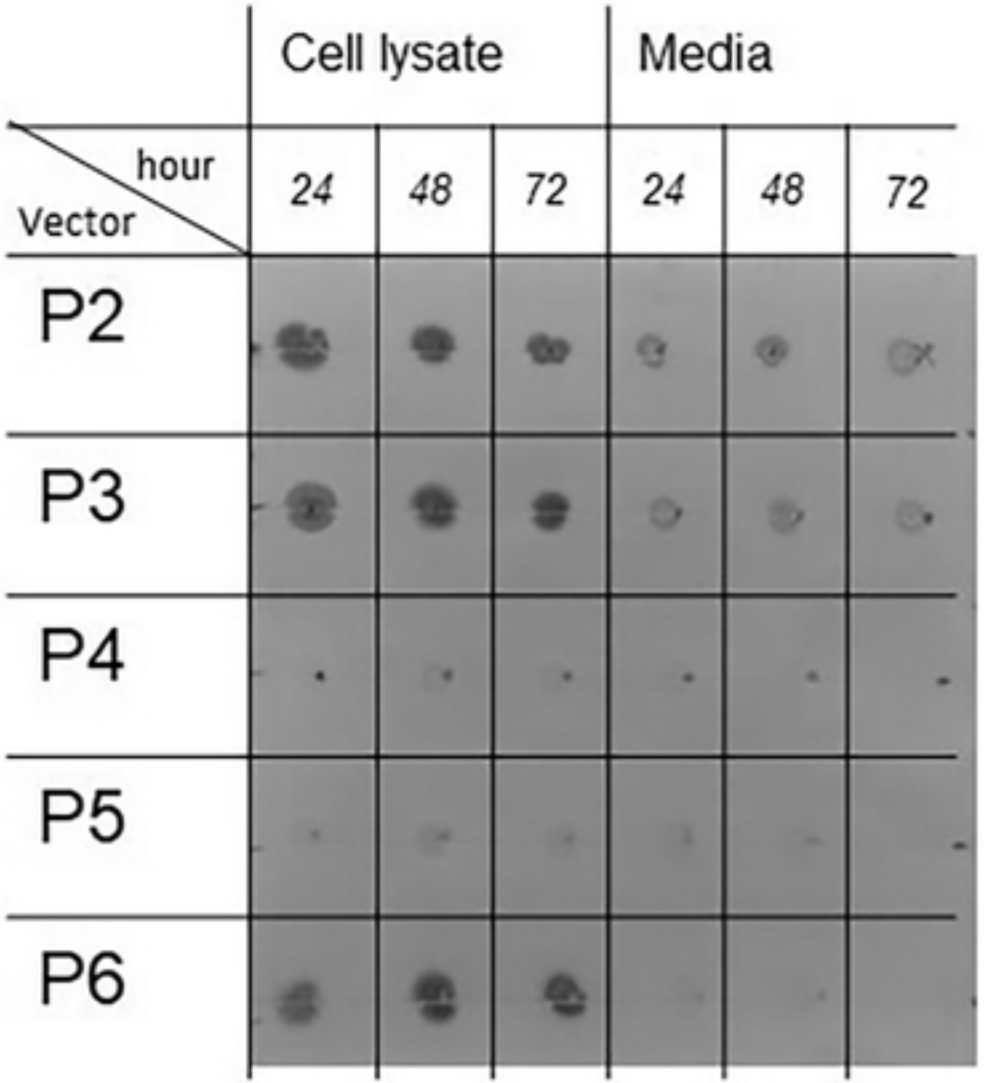
Cell lysate
Media
hour
Vector
24
48
72
24
48
72
P2
P3
P4
P5
P6

Figure 2

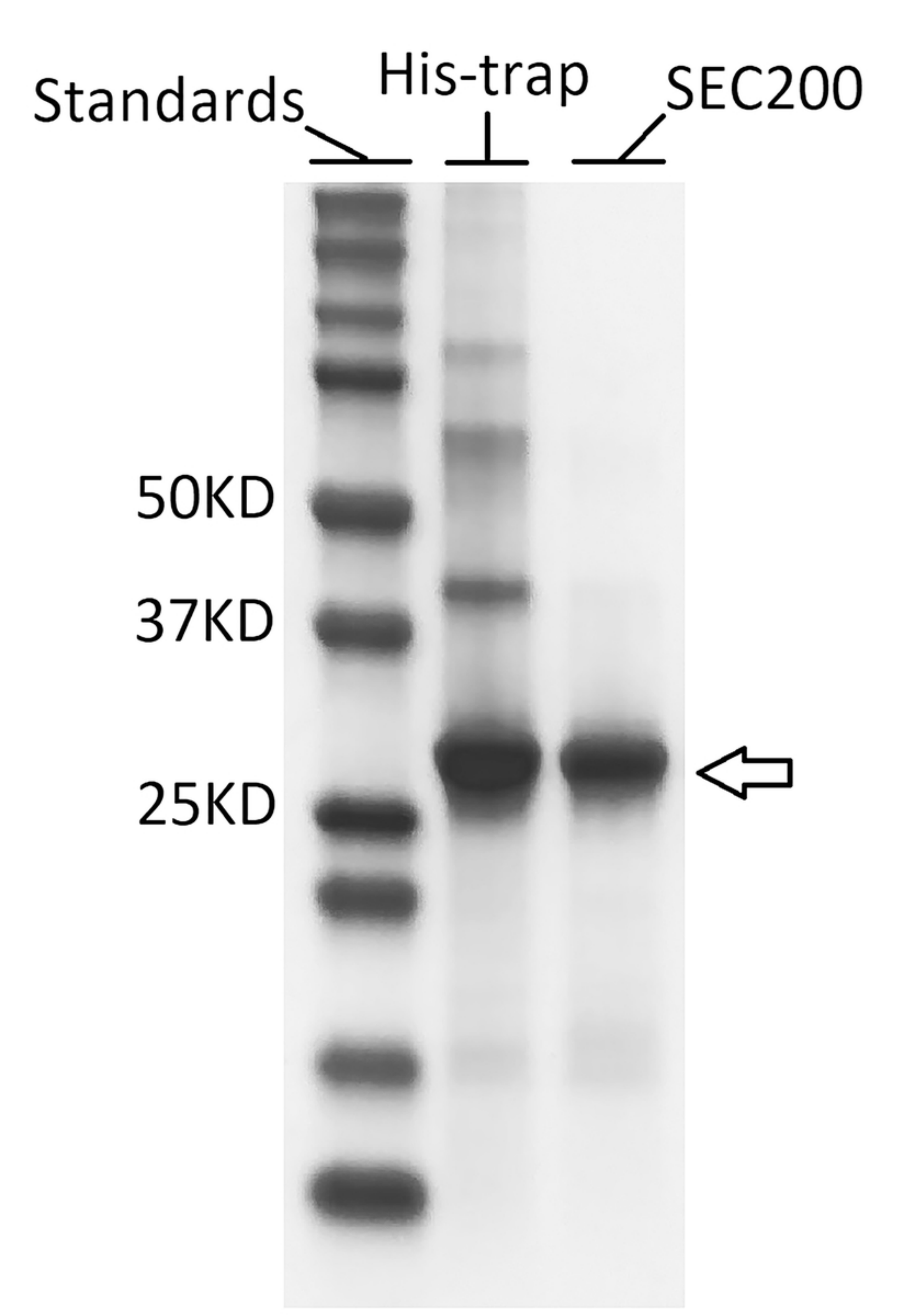

Figure 3

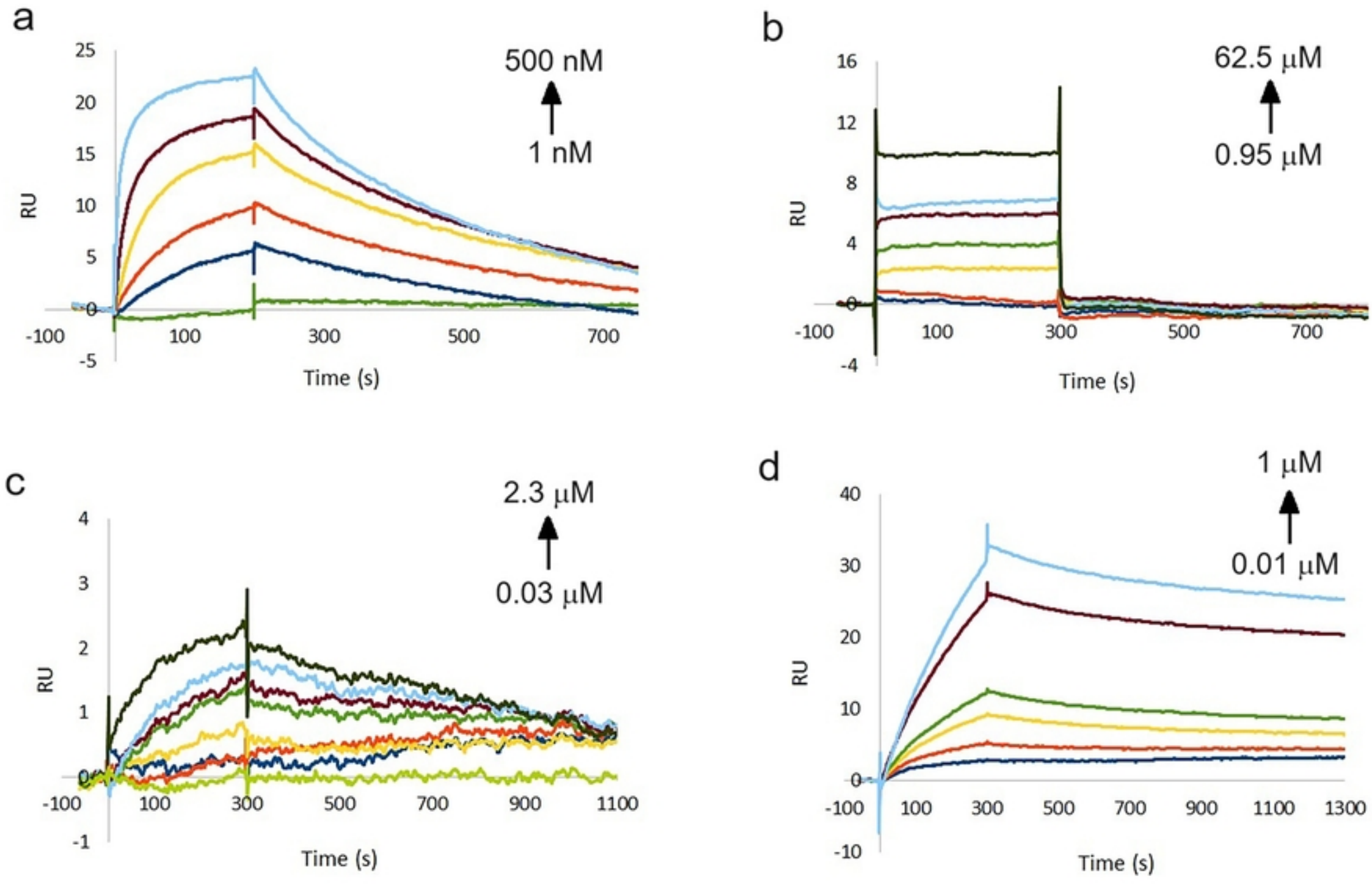
a
500 nM
1 nM
RU
Time (s)
b
62.5 μM
0.95 μM
RU
Time (s)
c
2.3 μM
0.03 μM
RU
Time (s)
d
1 μM
0.01 μM
RU
Time (s)

Figure 4